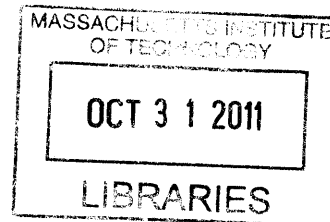# A Quantum Top in a Casimir-Induced Quadrupole Field

by

Eric Andrew Vitus Fitzgerald

B.S., University of Oregon (2003)

Submitted to the Department of Physics
in partial fulfillment of the requirements for the degree of

Master of Science in Physics

at the

MASSACHUSETTS INSTITUTE OF TECHNOLOGY

May 2011
[June 2011]

Author . . . .
Department of Physics
May 6, 2011

Certified by. . . . .
Robert L. Jaffe
Jane and Otto Morningstar Professor of Physics
Thesis Supervisor

Accepted by . . . .
Krishna Rajagopal
Associate Department Head for Education

A Quantum Top in a Casimir-Induced Quadrupole Field

by

Eric Andrew Vitus Fitzgerald

Submitted to the Department of Physics
on May 6, 2011, in partial fulfillment of the
requirements for the degree of
Master of Science in Physics

Abstract

The Casimir energy is the change in energy of a configuration of objects due to second quantization of the electromagnetic field. The Casimir energy of a dielectric object inside a perfectly conducting sphere was recently analyzed [1]. Building on this result, I calculate the changes in energy levels of a quantum top inside a cavity after promoting the Casimir energy to a quantum Hamiltonian. I apply the result to a diatomic molecule and find the changes in the spectroscopy induced by the Casimir effect. This can potentially provide an additional experimental probe into the Casimir effect.

Thesis Supervisor: Robert L. Jaffe
Title: Jane and Otto Morningstar Professor of Physics

Acknowledgments

A very deep and heartfelt thanks to professor Robert Jaffe, without whose guidance, support, assurance, and reassurance, I would not be finishing this thesis.

I must thank all of my friends and officemates throughout my time here. Vijay, Claudio, Andy, Andrea, Dave, Tom, Mark, Nabil, Christiana, Brian, Alan, Adam, Ben, Andrew, Robyn... Too many to count, and all great friends and supporters. Really, to all my friends. Ashley, Andrew, Jake, Nels, Ben, Joe, Joseph, Sydney, Pete, Katie, Dan, Beau, Michael... We're the product of all the interactions we've had in the universe, and I count myself lucky to have interacted with all of you. And to my brother, Tim, who beat me to a Masters despite being three years younger.

To Tom and Marianne. Thank you for being my parents. There is not enough thanks in the world for all the love and support that you've given me over the years.

And to Stephanie, the light and love of my life.

"O Lady! thou in whom my hopes have rest;

Who, for my safety, hast not scornd, in Hell

To leave the traces of thy footsteps markd;

for all mine eyes have seen, I to thy power

And goodness, virtue owe and grace. Of slave

Thou hast to freedom brought me: and no means,

For my deliverance apt, hast left untried.

Thy liberal bounty still toward me keep:

That, when my spirit, which thou madest whole,

Is loosend from this body, it may find

Favour with thee."

— Dante Alighieri, *Paradiso*, Canto XXXI, Lines 71-81

3

Chapter 1

Introduction

Casimir energies arise from quantum fluctuations of the electromagnetic (EM) field modified by the presence of objects [2, 3, 4, 5, 6]. The fluctuating EM field must obey boundary conditions imposed by the objects. The boundary conditions depend on the size, shape, spatial orientation, and EM frequency response of the objects. The Casimir energy is the difference between the energy in the EM field with the objects present and with the objects infinitely separated.

Recently a novel technique for computing the Casimir energy was developed based on scattering theory [4, 5, 6]. This method uses scattering amplitudes originating at the surface of the objects and translation matrices that propagate the fluctuations through the EM field. The scattering amplitudes encode the objects' spatial geometry and EM properties, and the translation matrices encode their relative orientations and separations. These methods have been used to precisely calculate Casimir energies for a variety of configurations of both conductors and dielectrics. Precision experiments measuring Casimir forces in the laboratory have provided tests for these new theoretical tools [7].

I will apply the results of Zaheer et al. [1] — that of a polarizable dielectric inside a perfectly conducting sphere — to the energy levels of a quantum top. They calculated the Casimir energy as a function of the classical coordinates (the location and orientation) of an object inside a sphere. I will elevate this to a quantum Hamiltonian in the space of states of the quantized top. This is justified by a separation of

scales: the fluctuations that dominate the Casimir energy are much faster than the motion of the top. Treating the top as stationary, it is sensible to use an adiabatic approximation where the Casimir effect is a small perturbation on the energy levels of the top.

First I review the general method for computing the Casimir energy as well as the result for a polarizable material inside a conducting sphere. Next I review the quantum top, including the quantum numbers, energy eigenvalues, and wavefunctions. Then I treat the Casimir energy as a first-quantized Hamiltonian and apply first-order perturbation theory to a quantum top. Last, I use these results to study changes to the spectroscopy of a diatomic molecule. Current experiments study the Casimir effect using molecular force probes and other microelectromechanical devices; precision spectroscopy can provide an additional experimental test of these Casimir energies.

Chapter 2

The Classical Casimir Problem

The computational method for finding the Casimir energy uses a path integral formulation and techniques from scattering theory. I will outline the path integral method first. The action in the path integral uses the EM Lagrangian, and the functional integration is over all possible configurations of the EM fields subject to the constraints imposed by the objects. There are no free charges or currents, but quantum fluctuations induce currents inside and at the surfaces of the objects subject to the constraints imposed by the properties of the material. The constraints depend on the size, shape, and composition of the objects being studied. To find the energy, I start with the path integral formulation for the trace of the propagator.

$$\mathrm{Tr}\; e^{-iH_C T/\hbar} = \int [\mathcal{D}A]_{\mathcal{C}} \; \exp\left(\frac{i}{\hbar} S_{EM}(A)\right)$$

The subscript $\mathcal{C}$ denotes the constraints imposed by the objects. The EM action depends on the total time elapsed T and the fields $\vec{E}$ and $\vec{B}$.

$$S_{EM}(A, T) = \frac{T}{2} \sum_{n=-\infty}^{+\infty} \int d^3x \left(\epsilon \vec{E}^* \cdot \vec{E} - \frac{1}{\mu} \vec{B}^* \cdot \vec{B}\right)$$

The EM fields, as well as the permittivity ϵ and permeability μ, depend on both position $\vec{x}$ and frequency $\omega_n = \frac{2\pi n}{T}$.

The partition function for a system at temperature $T = \frac{1}{\beta}$ is defined by the trace

over the states weighted by $e^{-\beta H}$,

$$Z(\beta) \equiv \mathrm{Tr}\ e^{-\beta H}.$$

The free energy for the system is

$$F(\beta) = -\frac{1}{\beta} \log Z(\beta).$$

The ground-state energy is projected out by taking the limit $\beta \to \infty$,

$$\mathcal{E}_0 = -\lim_{\beta \to \infty} \frac{1}{\beta} \log Z(\beta).$$

This energy will generally depend on an ultraviolet cutoff. However I am only interested in the energy due to the presence of the objects; by subtracting out a reference configuration Z_R, these divergences can be canceled. This is usually accomplished by separating the objects to infinity. When the objects are inside one another the reference configuration will be different, such as a concentric configuration (see [1]).

$$\mathcal{E} = -\lim_{\beta \to \infty} \frac{1}{\beta} \log Z(\beta)/Z_R(\beta)$$

Analytically continuing the time $T \to -i\hbar\beta$ in the EM action, the Minkowski path integral transforms into a Euclidean path integral. The trace of the Euclidean path integral is a partition function. Under this transformation, the frequency ω_n changes to the wavenumber $\kappa_n = \frac{2\pi n}{\hbar c \beta}$. The Lagrangian is quadratic, so modes with different κ_n decouple and the total partition function decomposes into a product of the partition function of each mode. The free energy is the logarithm of the total partition function divided by β; the logarithm of the product over all modes of the partition functions turns into a sum over all modes of the logarithm of the partition function of each mode. The ground-state energy is the free energy after taking the

7

limit $\beta \to \infty$. This limit turns the sum over all modes into the integral $\frac{\hbar c \beta}{2\pi} \int d\kappa$.

$$\mathcal{E} = -\frac{\hbar c}{2\pi} \int_0^\infty d\kappa \ \log Z(\kappa)/Z_R(\kappa) \tag{2.1}$$

This outlines a rather formal description of the Casimir energy, but to calculate it for a real system more practical techniques must be developed. The Casimir energy arises from the interaction of the currents and fields between the objects. The interactions between the currents can be expanded in multipoles, and the multipoles become the variables in the functional integral. These multipoles characterize the fluctuating potentials within and between objects and the corresponding surface currents on the objects that satisfy the appropriate boundary conditions. Calculating the interactions between these multipoles involves changing coordinate systems and translating between their respective origins. This can be expressed by a set of translation matrices, denoted $\mathbb{U}$. These translation matrices are universal — they are independent of the shape and composition of the objects — and only depend on the type of multipole expansion used and the relative position and orientation of the objects.

The self-interaction terms are the outgoing multipoles generated by the fluctuating surface currents on the object. This is defined in scattering theory as the $\mathbb{T}$-matrix and depends on the shape and composition of the object. As an example, consider the Casimir effect for two objects. There are two translation matrices, $\{\mathbb{U}^+, \mathbb{U}^-\}$, and two $\mathbb{T}$ matrices, $\{\mathbb{T}^1, \mathbb{T}^2\}$. $\mathbb{U}^+$ translates from object 1 to object 2; $\mathbb{U}^-$ translates from object 2 to object 1. $\mathbb{T}^1$ and $\mathbb{T}^2$ describe the outgoing fluctuations emanating from objects 1 and 2, respectively. After performing the outlined steps on the partition function using the effective action and multipoles, this becomes the two-body Casimir energy in (2.1):

$$\mathcal{E} = \frac{\hbar c}{2\pi} \int_0^\infty d\kappa \ \log \mathrm{Det}[1 - \mathbb{U}^- \mathbb{T}^2 \mathbb{U}^+ \mathbb{T}^1].$$

Defining a new matrix $\mathbb{N} \equiv \mathbb{U}^- \mathbb{T}^2 \mathbb{U}^+ \mathbb{T}^1$, using the matrix identity $\log \mathrm{Det} A = \mathrm{Tr} \log A$,

8

and expanding the logarithm as an infinite series, the Casimir energy becomes

$$\mathcal{E} = -\frac{\hbar c}{2\pi} \int d\kappa \, \text{Tr} \sum_{p=1}^{\infty} \frac{1}{p} \mathbb{N}^p. \tag{2.2}$$

This presents a simple physical interpretation. Each order in $\mathbb{N}$ generates a wave from the first object, travels to the second object, and is scattered back to the first object — an expansion in the number of two-scattering processes. Within $\mathbb{N}$ the matrices are built of multipoles that can be expanded as partial waves. This allows for controlled expansions of the Casimir energy to a desired accuracy.

Utilizing this formulation of the Casimir energy, Zaheer et al [1] calculated the Casimir energy of an object of size r inside a spherical metal shell of radius R. They summed all orders in the expansion of the logarithm in (2.2) but assumed the object to be small enough that only dipole fluctuations on the object contribute. This is the interior analog of the Casimir-Polder approximation [3]. In this limit the object's properties are summarized entirely by its static electric and magnetic polarizabilities. To leading order in the limit $R \gg r$, they found the Casimir energy as a function of the displacement of the object from the center of the sphere to be

$$\mathcal{E} = \frac{\hbar c}{3\pi R^4} \sum_{P=E,M} \left\{ (f^P(a/R) - f^P(0)) \text{Tr} \, \alpha^P + g^P(a/R)(2\alpha_{zz}^P - \alpha_{xx}^P - \alpha_{yy}^P) \right\}. \tag{2.3}$$

The functions f and g are known in terms of modified Bessel functions. Generally, the f-function is about an order of magnitude larger than the g-function for a given displacement $\frac{a}{R}$. The tensor α^P is the static electric ($P = E$) or magnetic ($P = M$) polarizability tensor of the object. The most interesting features of this formula are the non-trivial dependence on the displacement and the orientation dependence of the coupling to the polarizability tensor.
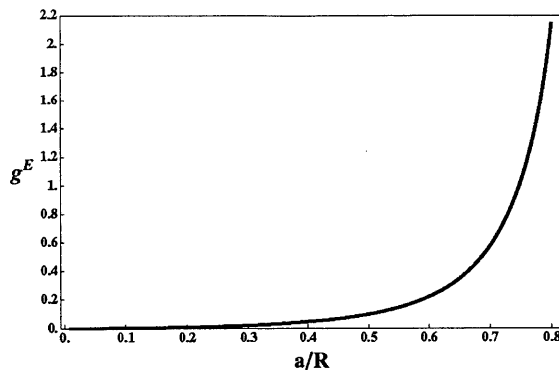
9

Figure 2-1: g^E as a function of displacement from the center of the sphere. The other coefficient function g^M is positive and follows a similar functional form. The f coefficient functions follow a similar functional form and are both larger by roughly an order of magnitude, with f^M positive and f^E negative.

2.1 Adiabatic Quantization of Motion in a Casimir "Potential"

The Casimir energy in (2.3) is a quantum mechanical effect that comes from the second quantization of the EM field. However, this result is a "classical" energy in the sense that it treats the object as fixed in space and orientation. In this thesis I explore treating this energy as a quantum Hamiltonian acting on a quantized top using perturbation theory. The Casimir energy is dominated by contributions to the wavenumber integration in the $\kappa \sim \frac{1}{R}$ region for a cavity of radius R. The quantum top rotates at a frequency dependent on the total angular momentum and principle moments of inertia of the top. In order for the calculation to be valid in the quantum situation, the top must be treated as effectively static and adiabatically responsive to the Casimir effect. This requires the quantum timescale associated with the rotation of the top to be sufficiently greater than the timescales that dominate the Casimir effect. The rotational energy is $\frac{1}{2}I\omega_{rot}^2 = \frac{J^2}{2I}$, and the semi-classical rotational frequency is estimated by $\omega_{rot} = \frac{\hbar}{I}\sqrt{J(J+1)}$. The dominant frequency from the Casimir effect is approximately $\omega_{cas} \sim \frac{c}{R}$. The requirement $\omega_{cas} \gg \omega_{rot}$ gives this condition on the cavity radius in terms of the characteristic moment of inertia of the

10

top,

$$\frac{cI}{\hbar\sqrt{J(J+1)}} \gg R. \tag{2.4}$$

If the cavity radius satisfies this requirement, then both the low-frequency approximation used to derive the energy formula and first-order perturbation theory are valid. For a physical system such as a diatomic molecule this is easily satisfied.

2.2 Static Polarizability Tensor Components in Different Frames

The polarizability tensor that appears in the Casimir energy 2.3 is the static electric/magnetic polarizability of the object. This is defined in terms of the response of the object to a constant external electric/magnetic field. The polarizability tensor is the coefficient matrix from the first correction of the potential due to the presence of the object; there are higher-order tensors that can contribute as well. The polarizability is measured in the static limit.

$$\Phi = \vec{r} \cdot \vec{E}_{ext} + \frac{\vec{r} \cdot \alpha^E \cdot \vec{E}_{ext}}{r^3} + \cdots$$

This is a symmetric rank-2 Cartesian tensor, and it forms a reducible representation under the angular momentum algebra. In the angular momentum algebra, the polarizability can have spherical tensor components of rank-0, 1, or 2. Because it is symmetric in the Cartesian basis, the rank-1 components vanish. The rank-0 component is a scalar under rotations. Therefore the orientation dependence of the object is found in the rank-2 components. The spherical tensor components for the polarizability will be designated $[T_\alpha]_m^{(L)}$.

The body frame of the object is chosen so that the polarizability tensor is diagonal in the Cartesian basis, leaving three free quantities $\alpha_{11}^0, \alpha_{22}^0,$ and α_{33}^0, where the EM label is supressed. I define three new combinations of these, $\alpha = \alpha_{11}^0 + \alpha_{22}^0 + \alpha_{33}^0 =$

$\text{Tr}\,\alpha^0$, $\beta = \alpha^0_{11} - \alpha^0_{22}$, and $\gamma = \alpha^0_{33} - \frac{1}{2}(\alpha^0_{11} + \alpha^0_{22})$. The quantities α, β, and γ are defined in terms of the body frame cartesian components. The first, α, is the $L = 0$ spherical tensor component and is a scalar under rotations. The remaining two, β and γ, correspond to the $L = 2$ components.

$$
\begin{aligned}
\left[T_\alpha^{body}\right]_0^{(2)} &\equiv \sqrt{\tfrac{2}{3}}\gamma &&= -\sqrt{\tfrac{1}{6}}(2\alpha^0_{33} - \alpha^0_{11} - \alpha^0_{22}) \\
\left[T_\alpha^{body}\right]_{\pm 2}^{(2)} &\equiv \tfrac{1}{2}\beta &&= \tfrac{1}{2}(\alpha^0_{11} - \alpha^0_{22})
\end{aligned}
\tag{2.5}
$$

I select this normalization for later convenience. These components are in a special frame where the tensor is diagonal. To distinguish between the polarizability components in the different frames, I use numbers in the subscripts (e.g. α_{33}) to designate the body frame and letters (e.g. α_{zz}) to designate any external (lab) frame.

To rotate the polarizability tensor from one frame into a different frame, a set of Euler angles denoted $\omega = (\phi, \theta, \chi)$ can be used. These rotations can be performed by use of the Wigner $\mathcal{D}$ functions (see appendix A.2). I follow the conventions defined in Edmunds [8].

$$
[T_\alpha]_m^{(2)} = \sum_{m'=-2}^{2} \mathcal{D}^{(2)}_{m,m'}(\phi, \theta, \chi)\,[T'_\alpha]_{m'}^{(2)} = \sum_{m'=-2}^{2} e^{-im\chi} d^{(2)}_{m,m'}(\theta) e^{-im'\phi}\,[T'_\alpha]_{m'}^{(2)}
$$

The Casimir energy in (2.3) only couples to the $L = 0$ and $L = 2$, $m = 0$ components of the polarizability tensor in the frame of the cavity. This is defined by the choice of the z-axis to be the axis of displacement of the object inside the sphere. To find the Casimir energy due to the object inside the sphere at an arbitrary orientation, I rotate the body frame components into the frame of the cavity.

$$
\left[T_\alpha^{lab}\right]_0^{(2)} = \sum_{m'=-2}^{2} d^{(2)}_{0,m'}(\theta) e^{-im'\phi}\left[T_\alpha^{body}\right]_{m'}^{(2)} = \frac{1}{\sqrt{6}}\left[\frac{3}{2}\beta \sin^2\theta \cos 2\phi + \gamma(3\cos^2\theta - 1)\right]
$$

The scalar component is the same in both frames. The energy can be expressed in

terms of α, β, and γ and the orientation of the object relative to the lab frame.

$$\mathcal{E} = \frac{\hbar c}{3\pi R^4} \sum_{P=E,M} \left\{ (f^P(a/R) - f^P(0)) \left[T_{\alpha^P}^{lab} \right]_0^{(0)} + g^P(a/R) \left[T_{\alpha^P}^{lab} \right]_0^{(2)} \right\}. \qquad (2.6)$$

Chapter 3

The Quantum Top

The classical kinetic energy for a free top is

$$T = \frac{1}{2}I_1\omega_1^2 + \frac{1}{2}I_2\omega_2^2 + \frac{1}{2}I_3\omega_3^2.$$

The I_i are the diagonal components of the moment of inertia tensor in the body frame of the object, and the ω_i are the corresponding rotational velocities about the body frame axes. In this frame the conjugate momenta are $J_i = I_i\omega_i$, and the kinetic energy is

$$T = \frac{J_1^2}{2I_1} + \frac{J_2^2}{2I_2} + \frac{J_3^2}{2I_3}.$$

This is the classical Hamiltonian for a free top, which can now be quantized canonically. In this case the quantization of angular momentum is slightly modified from the standard fixed-axes angular momentum. The coordinate system for the angular momentum is in the body frame, so the axes are rotating with the top. This introduces an additional minus sign in the commutation relations, $[J_i, J_j] = -i\epsilon_{ijk}J_k$. This is still an angular momentum algebra, and all the standard results apply if the minus sign is treated carefully. The quantum operators $\hat{J}^2$ and $\hat{J}_3$ can still be diagonalized normally. The eigenvalues are $\hbar^2 J(J+1)$ and $\hbar K$ respectively, with ranges $J \geq 0$ and $-J \leq K \leq J$. In addition to diagonalizing along $\hat{J}_3$, it is possible to simultaneously

diagonalize along one of the external frame coordinates, $\hat{J}_z$. This follows from the fact that $\hat{J}^2$ and $\hat{J}_z$ both commute with the operator $\hat{J}_3 = \hat{J} \cdot \hat{n}_3$, where $\hat{n}_3$ is the unit vector along the principle 3-axis. The product $\hat{J} \cdot \hat{n}_3$ is a scalar with respect to rotations of the top and is independent of any external coordinate rotations generated by $\hat{J}$ or $\hat{J}_z$. The eigenvalues of $\hat{J}_z$ are $\hbar M$ with $-J \leq M \leq J$.

3.1 The Symmetric Top

The simplest example of a quantum top is a rigid sphere, where the moment of inertia for all three axes are equal, so $I_1 = I_2 = I_3$. In this case the Hamiltonian is $\hat{H} = \frac{1}{2I}\hat{J}^2$. The energy levels are $E = \frac{\hbar^2}{2I}J(J + 1)$. Each level is $(2J + 1)^2$ degenerate, with a factor of $(2J + 1)$ for both quantum numbers M and K. In this example the Casimir energy is orientation independent because the sphere has no preferred direction.

A symmetric top has axial symmetry with principle moments $I_1 = I_2 \neq I_3$. Adding and subtracting the term $\frac{\hat{J}_3^2}{2I_1}$ from the Hamiltonian rewrites it in terms of the operators $\hat{J}^2$ and $\hat{J}_3$.

$$\hat{H} = \frac{\hat{J}^2}{2I_1} + \frac{1}{2}\left(\frac{1}{I_3} - \frac{1}{I_1}\right)\hat{J}_3^2 = \frac{1}{2I_1}\left(\hat{J}^2 + (\epsilon - 1)\hat{J}_3^2\right)$$

The parameter $\epsilon \equiv \frac{I_1}{I_3}$ characterizes the shape of the top. This is always positive — when $\epsilon > 1$ the top is prolate (cigar-like) and when $\epsilon < 1$ the top is oblate (pancake-like). In a basis of the operators $\hat{J}^2$, $\hat{J}_3$, and $\hat{J}_z$, the energy levels are

$$E = \frac{\hbar^2}{2I_1}(J(J + 1) + (\epsilon - 1)K^2). \tag{3.1}$$

The states with $K = 0$ are non-degenerate. The states with $K \neq 0$ are doubly degenerate between the $\pm K$ states. All of the states are still degenerate for all $(2J + 1)$ M-values. The Wigner $\mathcal{D}$ functions are the rotational wavefunctions and the rotational coordinates are the Euler angles ω.

$$\psi_{MK}^{(J)}(\omega) = \langle \omega | J, M, K \rangle = \sqrt{\frac{2J + 1}{8\pi^2}}\mathcal{D}_{MK}^{(J)}(\omega)$$
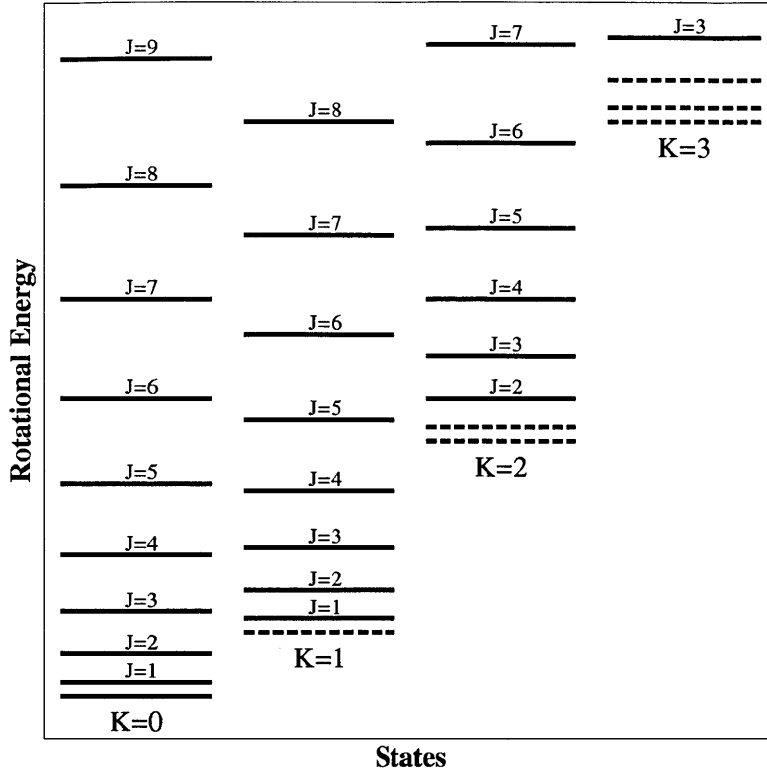
Figure 3-1: Energy levels for the quantum top, with $\epsilon = 10$. The dotted lines indicate levels forbidden because $J < K$.

These wavefunctions are normalized over the space of the Euler angles. The measure over this space is $d\omega = \sin\theta\, d\phi\, d\theta\, d\chi$ and the total solid angle is $8\pi^2$. When $K = 0$, the eigenfunction is independent of the orientation of the 3-axis and the $\mathcal{D}$ functions reduce to the standard spherical harmonics.

$$\psi^{(J)}_{M,K=0}(\omega) = \frac{(-1)^M}{\sqrt{2\pi}} Y_{JM}(\theta,\phi) \tag{3.2}$$

The factor $(-1)^M$ follows from the choice of phase and the $\frac{1}{\sqrt{2\pi}}$ factor normalizes the wavefunction with respect to the χ angle.

Until now I have assumed that the top was a rigid, featureless object. However, if there is some structure to the top, an additional component of the wavefunction can be included along with the associated quantum numbers. I designate this internal

16

wavefunction $\Phi(Q)$.

$$\Psi_{MK}^{(J)}(\omega, Q) = \sqrt{\frac{2J+1}{8\pi^2}} \mathcal{D}_{MK}^{(J)}(\omega)\Phi(Q) \tag{3.3}$$

3.2 Discrete Symmetries of the Symmetric Top

A symmetric top can be characterized by two discrete symmetries [9, 10, 11]. One of these is parity, the inversion of the external frame coordinates. The other is an exchange symmetry, which indicates the top is symmetric about a reflection in the xy-plane that divides the upper and lower halves of the top.

3.2.1 Parity

Under the parity operation the external coordinates are inverted. The first two Euler angles are spherical polar angles that follow the well-known transformation under parity of $\phi \to \pi + \phi$ and $\theta \to \pi - \theta$. The third Euler angle, χ, is a rotation about the final z-axis. However, the symmetric top is identical under rotations about the internal 3-axis, meaning the final rotation is redundant. I rotate the internal 2-axis so that it matches its alignment before the parity inversion, a convention that will be useful for the other discrete symmetry. This is accomplished with the transformation $\chi \to \pi - \chi$. I will show how this affects the wavefunction assuming that the internal wavefunction is an eigenfunction of parity, $\mathcal{P}\Phi(Q) = p\Phi(Q)$, where $p = \pm 1$. In the $K = 0$ case the rotational wavefunctions reduce to the spherical harmonics (3.2), which are eigenstates of parity with eigenvalue $(-1)^J$. The total parity of the state is $\pi = p(-1)^J$, and the wavefunction is

$$\Psi_{M,K=0,\pi}^{(J)}(\omega) = \frac{(-1)^M}{\sqrt{2\pi}} Y_{JM}(\theta, \phi)\Phi(Q) \ . \tag{3.4}$$

The parity alternates between the J states. If the internal function is not an eigenfunction of parity, one can be constructed from a linear combination of the states $\Phi(Q)$ and $\mathcal{P}\Phi(Q) = \tilde{\Phi}(Q)$.

In the $K \neq 0$ case, the rotational wavefunctions are not eigenstates of parity. I calculate how the wavefunctions change under this transformation, assuming the internal wavefunction transforms as $\mathcal{P}\Phi(Q) = \tilde{\Phi}(Q)$.

$$
\begin{aligned}
\mathcal{P}\Psi_{MK}^{(J)}(\omega) &= \left(\frac{2J+1}{8\pi^2}\right)^{1/2} \mathcal{D}_{MK}^{(J)}(\pi + \phi, \pi - \theta, \pi - \chi)\tilde{\Phi}(Q) \\
&= (-1)^{J-K}\left(\frac{2J+1}{8\pi^2}\right)^{1/2} \mathcal{D}_{M,-K}^{(J)}(\omega)\tilde{\Phi}(Q)
\end{aligned}
$$

This changes the sign of K, changes the internal wavefunction to $\tilde{\Phi}(Q)$, and introduces an overall sign of $(-1)^{J-K}$. States of definite parity are constructed from the pair of degenerate states with $\pm K$.

$$
\Psi_{MK,\pi=\pm}^{(J)}(\omega) = \left(\frac{2J+1}{16\pi^2}\right)^{1/2}\left[\mathcal{D}_{M,K}^{(J)}(\omega)\Phi(Q) \pm (-1)^{J-K}\mathcal{D}_{M,-K}^{(J)}(\omega)\tilde{\Phi}(Q)\right] \quad (3.5)
$$

3.2.2 $\mathcal{R}$-Symmetry

The second discrete symmetry is the exchange of the upper and lower halves of the top. In the top's body frame this is accomplished through the operator $\mathcal{R}_i$, a rotation by π about the internal 2-axis. In the lab frame this rotation is designated $\mathcal{R}_e$; it is identical to the rotation performed in the parity operation. If the top has this symmetry property, then these two operations must be identical. The two cases with $K = 0$ and $K \neq 0$ have important differences.

When $K = 0$, the operator $\mathcal{R}_i$ acts on the internal state $\Phi(Q)$ and has eigenvalues $r = \pm 1$. The eigenvalues must be ± 1 because $\mathcal{R}_i^2$ is a rotation by 2π for a system with integer angular momentum, and thus $\mathcal{R}_i^2 = +1$. The operator $\mathcal{R}_e$ acts on the rotational wavefunction in the same way as the parity operation due to the choice of transformation of χ. The eigenvalue is the same as before, $(-1)^J$. Setting the two

eigenvalues equal, the top has the following rotational spectrum:

$$\Psi^{(J)}_{M,0,r}(\omega) = \frac{(-1)^M}{\sqrt{2\pi}} Y_{JM}(\theta, \phi)\Phi(Q).$$

$$r = +1 \quad \Rightarrow \quad J = 0, 2, 4, \dots$$

$$r = -1 \quad \Rightarrow \quad J = 1, 3, 5, \dots$$

A top with an internal state that has a definite r-value has either $J = 0, 2, 4, \cdots$ or $J = 1, 3, 5, \cdots$. This is a powerful constraint on the rotational spectrum that halves the allowed J values based on the internal symmetry of the top. The eigenfunctions when $K = 0$ are the same for parity in equation (3.4), and the quantum numbers r and p are distinct.

When $K \neq 0$, the internal state can no longer necessarily be labeled with the eigenvalue r. Instead, I denote the rotated state $\mathcal{R}_i^{-1}\Phi(Q) \equiv \bar{\Phi}(Q)$. The operator $\mathcal{R}_i$ has the eigenvalues $\mathcal{R}_i^2 = (-1)^{2J}$. The internal state may not have integer total angular momentum and this operator introduces a complex phase instead of a real eigenvalue. The rotation $\mathcal{R}_e$ acts on the rotational wavefunction with the same transformation as parity. This operator introduces a phase $(-1)^{J-K}$ and takes $K \to -K$.

$$\Psi^{(J)}_{MK}(\omega) = \left(\frac{2J+1}{16\pi^2}\right)^{1/2} \left[\mathcal{D}^{(J)}_{M,K}(\omega)\Phi(Q) + (-1)^{J-K}\mathcal{D}^{(J)}_{M,-K}(\omega)\bar{\Phi}(Q)\right] \qquad (3.6)$$

The $\mathcal{P}$ and $\mathcal{R}$ operators acting on the rotational wavefunctions have the same effect on the Euler angles and thus are commuting observables. For the total wavefunction to be an eigenfunction of both, the internal wavefunction must transform such that $\tilde{\Phi}(Q) = \pm\bar{\Phi}(Q)$.

$K = 0$		$K \neq 0$
$r = +1, \pi = p$	$r = -1, \pi = -p$	$\pi = \pm 1$
$J = 0, 2, 4, \dots$	$J = 1, 3, 5, \dots$	$J = K, K+1, K+2, \dots$

Table 3.1: The allowed quantum numbers of the states of the top.

Chapter 4

The Casimir Effect on a

Quantum Top

Before calculating the matrix elements of the Casimir effect for a quantum top, an analogy can be drawn with the electric dipole operator for a charged particle on a sphere. In this case the wavefunction for the particle is described in terms of spherical harmonics Y_{lm} rather than Wigner $\mathcal{D}$ functions. The dipole moment operator is qz, where q is the charge of the particle and z is the displacement along the z-axis. The position operator z can be rewritten as $R\cos\theta$ since the particle is constrained to a sphere. In terms of spherical harmonics, this is proportional to Y_{10}.

$$
\begin{aligned}
\langle J', M'|qz|J, M\rangle &= \int d\Omega d\Omega' \langle J'M'|\Omega'\rangle\langle\Omega'|qR\cos\theta|\Omega\rangle\langle\Omega|J, M\rangle \\
&\sim qR \int d\Omega d\Omega'\, Y_{J'M'}(\Omega')\, Y_{10}(\Omega)\, \delta(\Omega - \Omega')\, Y_{JM}(\Omega) \\
&\sim qR \begin{pmatrix} J' & 1 & J \\ -M' & 0 & M \end{pmatrix}
\end{aligned}
$$

This matrix element evaluates to a reduced matrix element, qR, and a Wigner $3j$ symbol.

For a quantum top inside a conducting spherical cavity, I start with the Casimir energy found in equation (2.6). The polarizability tensor is promoted to a quantum

operator and the "classical" energy becomes the Hamiltonian operator. The coefficients for the different spherical tensor components are denoted $B_{L,m}^P$. I find the first-order energy splittings due to this interaction by taking the expectation value of the Hamiltonian between two states $\langle S' | \mathcal{H} | S \rangle$. These states are labeled with rotational quantum numbers $J^{(\prime)}$, $M^{(\prime)}$, and $K^{(\prime)}$. Let $Q^{(\prime)}$ denote any additional quantum numbers that characterize the system.

$$\langle S' | \mathcal{H} | S \rangle = \sum_{P,L,m} B_{L,m}^P \langle J', M', K', Q' | [T_{\alpha^P}]_m^L | J, M, K, Q \rangle$$

From equation (2.6), there are two non-zero coefficients, the $L = 0, m = 0$ scalar component and the $L = 2, m = 0$ tensor component. The scalar component is independent of the rotational configuration of the top; this shifts all of the states by a fixed amount and does not change the spectroscopy. The tensor component does depend on the rotational states and affects the rotational spectra, so the remaining analysis only includes that term. The coefficient for the $L = 2, m = 0$ polarizability operator is $B_{2,0}^P = \frac{\hbar c}{3\pi R^4} g^P(\frac{a}{R})$.

The classical polarizability is measured by fixing the object in space, applying a static uniform field, and measuring the response field. Let the $L = 2, m = 0$ quantum polarizability operator be denoted $[T_\alpha]_0^{(2)}$, where I suppress the electric/magnetic field index P. The object is held at the fixed Euler angle ω in the lab frame, and the expectation value for the polarizability is

$$\langle \omega' | [T_\alpha^{lab}]_0^{(2)} | \omega \rangle = [T_\alpha^{lab}]_0^{(2)} \delta(\omega' - \omega).$$

In section 2, I calculated the lab frame polarizability tensor in terms of the body frame components and Wigner $\mathcal{D}$ functions. To find the matrix element of the polarizability operator, I insert two complete sets of position states into the expectation value and use the expression for the integral of the product of three Wigner $\mathcal{D}$ functions to

21

evaluate the resulting integral (equation (A.2) in the appendix).

$$\langle S' | [T_\alpha^{lab}]_0^2 | S \rangle = \iint d\omega' d\omega \; \langle J', M', K' | \omega' \rangle \langle \omega' | [T_\alpha^{lab}]_0^{(2)} | \omega \rangle \langle \omega | J, M, K \rangle$$

$$= \iint d\omega d\omega' \sqrt{\frac{2J'+1}{8\pi^2}} \mathcal{D}_{M',K'}^{(J')*}(\omega') [T_\alpha^{lab}]_0^{(2)} \delta(\omega - \omega') \sqrt{\frac{2J+1}{8\pi^2}} \mathcal{D}_{M,K}^{(J)}(\omega)$$

$$= \frac{\sqrt{(2J'+1)(2J+1)}}{8\pi^2} \int d\omega \; \mathcal{D}_{M',K'}^{(J')*}(\omega) \times$$

$$\left(\sum_{m'} \mathcal{D}_{0,m'}^{(2)}(\omega) [T_\alpha^{body}]_{m'}^{(2)} \right) \mathcal{D}_{M,K}^{(J)}(\omega)$$

$$= (-1)^{K'-M'} \sqrt{(2J'+1)(2J+1)} \begin{pmatrix} J' & 2 & J \\ -M' & 0 & M \end{pmatrix} \times$$

$$\left[\sqrt{\frac{2}{3}} \gamma \begin{pmatrix} J' & 2 & J \\ -K' & 0 & K \end{pmatrix} + \frac{1}{2} \beta \begin{pmatrix} J' & 2 & J \\ -K' & +2 & K \end{pmatrix} + \frac{1}{2} \beta \begin{pmatrix} J' & 2 & J \\ -K' & -2 & K \end{pmatrix} \right]$$

In the last line I insert the combinations of the polarizability tensor defined in equation (2.5), $\beta = \alpha_{11}^0 - \alpha_{22}^0$ and $\gamma = \alpha_{33}^0 - \frac{1}{2}(\alpha_{11}^0 + \alpha_{22}^0)$, for the operators $[T_\alpha^{body}]_{\pm 2,0}^{(2)}$. The first Wigner $3j$ symbol gives the selection rule that $M = M'$ between the two states, which follows from how the Casimir effect couples to the polarizability. The z-axis is the axis of displacement of the top inside the sphere and M is the projection of the angular momentum this axis. Because the cavity is spherically symmetric, the coupling of the Casimir effect is independent of the z-axis and does not affect the M quantum number. The last line shows how the Casimir effect couples to the $L = 2$ polarizability tensor components. When the polarizability is axially symmetric the body frame components are $\alpha_{11}^0 = \alpha_{22}^0$, and the combinations are $\beta = 0$ and $\gamma = \alpha_{33}^0 - \alpha_{11}^0$. In this case, because the top is axially symmetric, only the first term in the final line contributes and gives the selection rule $K = K'$.

The first-order energy shift for the state $|J, M, K\rangle$ with an axially symmetric polarizability tensor is

$$\Delta E_{cas} = \sum_{P=E,M} B_{2,0}^P \sqrt{\frac{2}{3}} \gamma^P (-1)^{K-M} (2J+1) \begin{pmatrix} J & J & 2 \\ -M & M & 0 \end{pmatrix} \begin{pmatrix} J & J & 2 \\ -K & K & 0 \end{pmatrix}. \quad (4.1)$$

22

This is the shift in energy levels due to the Casimir effect for a polarizable symmetric top inside a conducting sphere. The sign of K does not affect the energy shift. The states with parity and/or $\mathcal{R}$ symmetry are superpositions of rotational eigenstates with quantum numbers $\pm K$, therefore these states will have the same change in energy levels. The free quantum top's energy levels are independent of the quantum number M. The perturbation due to the Casimir effect depends on the absolute value of the quantum number M, breaking the degeneracy. This result also follows from the Wigner-Eckart theorem by reducing along the M and K quantum numbers and assuming spherical symmetry of the cavity and axial symmetry of the top.
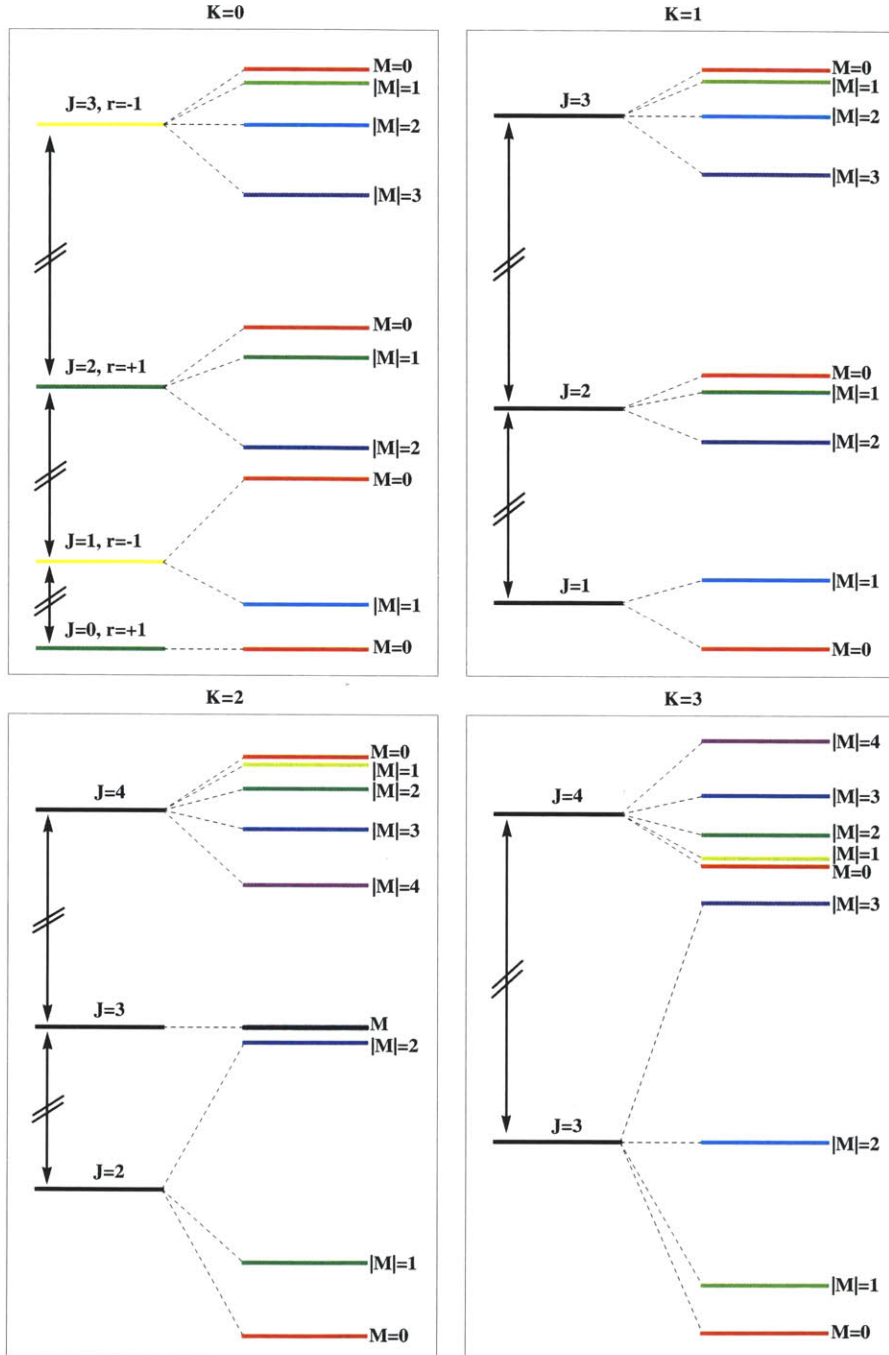
Figure 4-1: The Casimir splittings for the lower levels of the symmetric top. The spacing between the different splittings as a function of $|M|$ is to scale; the spacing between the different J states is not to scale. For example, in the $K = 2$ band the splitting between the highest and lowest $|M|$ states of the $J = 2$ states are approximately twice as large as the corresponding splitting of the $J = 4$ states. Due to a vanishing matrix element, the $K = 2$, $J = 3$ has no splitting. In the $K = 0$ band, the states with $r = +1$ have J even and are labeled in green, and states with $r = -1$ have J odd and are labeled in yellow.

Chapter 5

A Physical System —

Diatomic Molecules in a

Metallic Cavity

A diatomic molecule inside a metallic cavity provides an excellent test case for the Casimir effect. These molecules are axially symmetric tops, have well-known rotational band spectra, and have a non-zero $L = 2, M = 0$ spherical tensor component of their electric polarization. For a full discussion of the spectroscopy of diatomic molecules, see the classic text by Herzberg [9] or the modern Brown and Carrington [10].

5.1   Brief Review of Diatomic Spectroscopy

A diatomic molecule is a system of two nuclei and their respective electron cloud with a complicated set of interaction between every object involved. Even the simplest example of a hydrogen molecule does not permit an exact solution of the energy levels. In this case an adiabatic approximation is made, called the Born-Oppenheimer approximation, where the (fast-moving) electrons follow the motion of the (slow-moving) nuclei adiabatically. The electronic states change slowly from the motion of the nuclei and do not mix with each other. The electronic wavefunction depends

only on the position of the nuclei, not their momenta or orientation. The nuclear wavefunction neglects the electrons entirely; these interactions can mix the nuclear states. The electrons' positions are designated $\vec{r}_i$. The relative nuclear position and orientation is characterized by the inter-nuclear separation R and a set of Euler angles ω. This approximation separates the total wavefunction into a product of the electronic and nuclear wavefunctions.

$$\Psi_{\text{tot}} = \psi_e(R, \vec{r})\,\psi_N(R, \omega)$$

From here on I ignore the electronic wavefunction and assume that it is the ground state configuration. The two nuclei are bound by an inter-nuclear potential forming a "dumbbell" configuration that is free to rotate. At leading order, the rotational motion is that of a rigid, symmetric quantum top, and the binding potential is approximately a harmonic well. As a result, the wavefunction for the nuclei obeys a rotational-vibrational Schrödinger equation. An additional approximation assumes the rotational and vibrational motions are completely independent. This separates the nuclear wavefunction into rotational and vibrational components.

$$\psi_N(R, \omega) = \psi_{vib}^n(R)\,\psi_{rot}^n(\omega)$$

The vibrational wavefunction satisfies the harmonic oscillator wave equation, with vibrational modes denoted ν. There are higher-order anharmonic corrections to the potential function that can be treated perturbatively. Due to these corrections, the energy levels are treated as a perturbation series in the quantum number $(\nu + \frac{1}{2})$. Following standard spectroscopic notation, the first two coefficients are denoted ω_e and $-x_e\omega_e$.

$$\frac{E_{vib}}{hc} = \omega_e(\nu + 1/2) - x_e\omega_e(\nu + 1/2)^2 + \cdots$$

The coefficient $x_e\omega_e$ is approximately a factor of 10^{-2} smaller than ω_e.

The rotational wavefunction is a symmetric top, which is solved by the Wigner $\mathcal{D}$

26

functions as found in equation (3.3). The nuclei have two distinct moments of inertia, $I_\perp$ and $I_\parallel$, which are defined relative to the symmetry axis connecting the two nuclei of the molecule. These are assumed to be completely rigid. The body frame moments of inertia in Section 3 are $I_1 = I_2 = I_\perp$ and $I_3 = I_\parallel$. As the nuclei have much smaller radii than the inter-nuclear distance, $I_\perp \ggg I_\parallel$. Following standard spectroscopic notation, the two rotational coefficients are denoted $B = \frac{\hbar}{4\pi c I_\perp}$ and $A = \frac{\hbar}{4\pi c I_\parallel}$, with $A \ggg B$.

$$\frac{E_{rot}}{hc} = \frac{\hbar}{4\pi c I_\perp} J(J+1) + \left(\frac{\hbar}{4\pi c I_\parallel} - \frac{\hbar^2}{4\pi c I_\perp} \right) K^2 = BJ(J+1) + (A-B)K^2$$

Because $A \ggg B$, the states with different values of $|K|$ are completely separated from each other. The rotational energy levels are the same as those of a simple rotor, $BJ(J+1)$, except there is a shift of magnitude, $(A-B)K^2$, and levels with $J < K$ are absent [9]. The solution of the rotational wave equation assumes that the moment of inertia is perfectly rigid, however the nuclei are not at a fixed separation. Therefore the rotational constant B depends on the separation of the nuclei through the moment of inertia. There are numerous perturbative corrections that come from the rotational motion and the vibrational oscillations of the nuclei. Because of these corrections, the rotational energy levels are written as a power series in both the total angular momentum $J(J+1)$ and oscillator mode $(\nu + \frac{1}{2})$.

$$\frac{E_{rot}}{hc} = B_e J(J+1) - D_e J^2(J+1)^2 - \alpha_e J(J+1)(\nu+1/2) + \cdots \qquad (5.1)$$

The coefficients D_e and α_e are approximately 10^{-3} to 10^{-4} smaller than the rotational constant B_e.

In diatomic spectroscopy, the quantum number $|K|$ is designated Λ, with the notation $\{\Lambda = 0 \to \Sigma$ state, $\Lambda = 1 \to \Pi$ state, $\Lambda = 2 \to \Delta$ state, $\Lambda = 3 \to \Phi$ state, $\dots\}$. This is analogous to the spectroscopic notation for the electronic angular momentum of atomic states, $\{$S, P, D, F, $\dots\}$. For diatomic molecules, because they have axial symmetry instead of spherical symmetry, Λ is usually a good quantum number and is used to label the state. Depending on the strength

of the coupling between the nuclear and electronic degrees of freedom, the quantum number Σ for the projection of the total electronic angular momentum along the inter-nuclear axis is also needed. In this case the quantum number $\Omega = |\Lambda + \Sigma|$ is the good quantum number to label the states, however the notation labeling the states by $\{\Sigma, \Pi, \Delta, \Phi, \dots\}$ is maintained. The states are also labeled by the total spin angular momentum of the electronic wavefunction $\vec{S}_e$ with quantum number S. This is denoted by the combination $2S + 1$ in the upper-left index. The parity of the state is designated by $\pm$ in the upper-right index. For homo-nuclear molecules, there is an exchange symmetry between the two nuclei of the molecule. This is identical to the operator $\mathcal{R}$ discussed in section 3. In spectroscopic notation, the quantum number $r = \pm 1$ is instead denoted g and u for gerade ($r = +1$) and ungerade ($r = -1$), from the German for even and odd, and is placed in the lower-right index. For example, a parity even, gerade ground state with $S = 1/2$ and $\Omega = 0$ would be labeled $^2\Sigma_g^+$. Table 5.1 lists some diatomic molecules and their properties.

Molecule	Ground State [14]	Rotational Constant (B_e) (cm^{-1}) [14]	Polarizability [12, 13] (atomic units)		$(10^{-24}$ cm$^3)$
			$\alpha_\parallel^E$	$\alpha_\perp^E$	γ
H$_2$	$^1\Sigma_g^+$	60.85	6.8	4.8	.30
N$_2$	$^1\Sigma_g^+$	1.998	15	10	.74
O$_2$	$^3\Sigma_g^+$	1.438	15	8	1.0
Cl$_2$	$^1\Sigma_g^+$	0.244	64	17	7.0
HCl	$^1\Sigma^+$	10.59	24	22	.30
CO	$^1\Sigma^+$	1.931	15	12	.44
NO	$^2\Pi$	1.672	15	10	.74

Table 5.1: The ground state, rotational constant, and polarizability components of a selected set of diatomic molecules. The polarizabilities α are calculated in atomic units [12, 13]. The polarizability component that appears in the Casimir energy $\gamma = \alpha_\parallel - \alpha_\perp$ is in cm^3 to facilitate conversion to spectroscopic units.

5.2 The Adiabatic Condition

The adiabatic condition in equation (2.4) is in terms of the moment of inertia $I_\perp$. In terms of the rotational constant measured in spectroscopy, the adiabatic condition is

$$\frac{1}{4\pi B_e\sqrt{J(J+1)}} \gg R.$$

For the typical values of $B_e \sim 2$ cm^{-1} and $J \sim 20$, $\frac{1}{4\pi B_e\sqrt{J(J+1)}} = 2 \times 10^{-3}$ cm, and the adiabatic constraint is 20 μm $\gg R$. Chlorine may be the ideal molecule to study this effect — it has a very large polarizability and a very small rotational constant. For the chlorine molecule, the adiabatic constraint on the size of the cavity is 160 μm $\gg R$, a factor of 8 larger for the same J level. A larger cavity reduces the size of the energy splittings as $\frac{1}{R^4}$ but may be more experimentally realizable. The energy splittings grow linearly with the polarizability; chlorine's large polarizability can partially compensate for the lost energy sensitivity.

The size of the molecule is an additional constraint on the cavity. The calculation in [1] does not include the region near the cavity walls because higher-order fluctuations contribute and the sum over multipoles does not converge rapidly enough. To avoid this region the cavity should be much larger than the size of the molecule, $R \gg r$, which is about 10 Å.

5.3 Spectral Broadening

The Casimir effect induces a splitting of the $(2J+1)$ degenerate states due to the dependence on the M quantum number. The individual $|M|$ states may be difficult to resolve in precision spectroscopy; however, this could be measured as a broadening of the spectral lines. The broadening is the difference between the highest and lowest energy states split from the same initially degenerate J, K state. Some states have a small (or vanishing) broadening, while at large J all states broaden to an asymptotic value of $\frac{3}{4}$ times the coefficient $B_{2,0}\sqrt{\frac{2}{3}}\gamma$ from equation (4.1). Figure 5-1 shows how much the states broaden as a function of J within the same K band. For a cavity
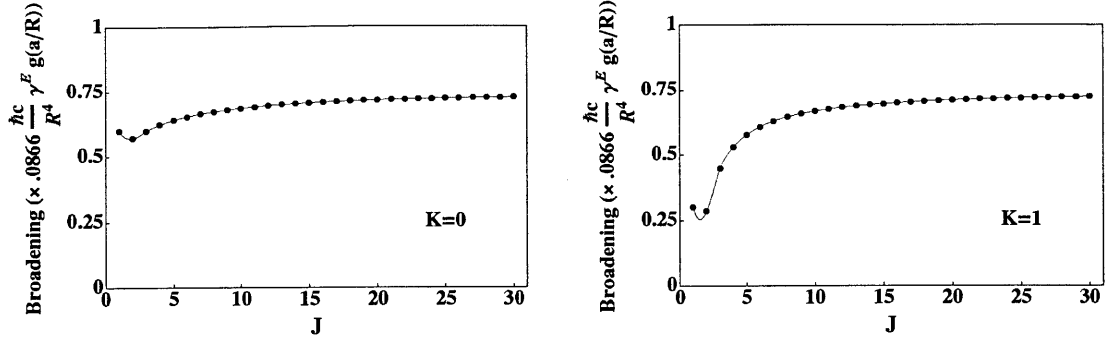
Figure 5-1: Broadening of the spectral lines as a function of J for the $K = 0$ and $K = 1$ bands. Higher K bands follow a similar pattern, and they all asymptote to a value of $\frac{3}{4}$ at large J.

radius of $R = 1$ μm and a molecule with polarizability 10^{-24} cm^3, a typical value of this broadening would be approximately 10^{-10} cm^{-1}, although this is very sensitive to the position in the cavity.

5.4 Dipole Transitions

The dominant transitions between rotational states are through dipole radiation. These transitions are proportional to the square of the matrix elements of the dipole moment operator, $\vec{\mu}_E = \mu_0(\hat{x} + \hat{y} + \hat{z})$, where μ_0 is the constant dipole moment of the molecule. To calculate the matrix elements, the direction operators are written in terms of the Wigner $\mathcal{D}$ functions.

$$\hat{x} = \frac{1}{\sqrt{2}}(\mathcal{D}^{(1)}_{1,0} - \mathcal{D}^{(1)}_{-1,0}) \ , \ \hat{y} = -\frac{i}{\sqrt{2}}(\mathcal{D}^{(1)}_{1,0} + \mathcal{D}^{(1)}_{-1,0}) \ , \ \hat{z} = \mathcal{D}^{(1)}_{0,0}$$

Inserting these into the dipole moment operator, the matrix elements are proportional to a set of Wigner $3j$ symbols.

$$\langle J', M', K' | \vec{\mu}_E | J, M, K \rangle \propto \begin{pmatrix} J' & 1 & J \\ K' & 0 & K \end{pmatrix} \times \begin{cases} \begin{pmatrix} J' & 1 & J \\ M' & \pm 1 & M \end{pmatrix} & \hat{x}, \hat{y} \\ \begin{pmatrix} J' & 1 & J \\ M' & 0 & M \end{pmatrix} & \hat{z} \end{cases}$$

30

The first Wigner $3j$ symbol requires $\Delta K = 0$, $\Delta J = 0, \pm 1$. If $K = 0$, then $\Delta J = 0$ is forbidden as well. The second Wigner $3j$ symbol has a similar set of conditions: $\Delta M = 0, \pm 1$ and $\Delta J = 0, \pm 1$. The molecule couples to all three of these cases and radiates in all directions. For a freely rotating diatomic molecule with fixed K, the energy levels are independent of M, and the frequency of radiation emitted is proportional to $J(J+1) - J'(J'+1)$. If $J' = J - 1$, the transition energy is

$$\frac{E}{hc} = B[J(J+1) - J(J-1)] = 2BJ.$$

The rotational spectrum lies in the 1 to 100 cm^{-1} range, depending on the molecule and transition. There are a variety of corrections to the spectrum from the rotational and vibrational motions (see equation (5.1)), which are smaller by a factor of 10^{-3} to 10^{-4}.

For a diatomic molecule inside a conducting cavity, the Casimir effect changes the rotational energy levels according to (4.1). The energy shift is of the same order as calculated for the spectral broadening in Table 5-1; for a cavity radius of $R = 1$ μm and molecule with polarizability 10^{-24} cm^3, the spectral change is approximately 10^{-10} cm^{-1}. The chlorine molecule can adiabatically respond to a much larger cavity. In this case, for a cavity of radius $R = 10$ μm and an estimated polarizability of 7×10^{-24} cm^3, the spectral change is approximately 10^{-13} cm^{-1}. The larger cavity radius reduces the spectral shift by four orders of magnitude. The extreme sensitivity of the Casimir energy on the cavity radius coupled with the adiabatic condition on the size of the cavity argues for a small cavity (e.g. $R < 1$ μm). This may present a difficult experimental challenge.

31

Chapter 6

Conclusion

I have calculated the Casimir energy splittings of a quantum top inside a perfectly conducting sphere. This required "adiabatic quantization" — treating the rotating top as effectively static and adiabatically responsive to the fluctuating electromagnetic field. The resulting Casimir energy depends on the static polarizability and all three quantum numbers (J, M, K) that describe the motion of the top. This perturbation induces a splitting in the rotational spectroscopy and breaks the degeneracy due to the quantum number M from $2J + 1$ to 2 states per rotational level. I applied the result to a diatomic molecule inside a metallic sphere, calculating the expected changes in spectroscopy in several diatomic systems. Though the experimental obstacles to measuring the small shifts calculated may be insurmountable for now, this can potentially provide an additional experimental test of the Casimir effect.

Appendix A

Selected Results from Edmonds'

Angular Momentum in

Quantum Mechanics

The following are a set of result from Edmonds' *Angular Momentum in Quantum Mechanics* [8], in particular from Chapters 3, 4, and 5. This was an invaluable text for my research as a clear, concise reference on the properties of the Wigner $3j$ symbols and the Wigner $\mathcal{D}$ functions, as well as the spherical tensors discussed in Chapter 2 and used throughout this thesis.

A.1 Wigner $3j$ Symbols

The Wigner $3j$ symbols come from the coupling of two angular momenta j_1 and j_2 to form a state with angular momentum j_3. The Wigner $3j$ symbols are defined by

$$
\begin{pmatrix} j_1 & j_2 & j_3 \\ m_1 & m_2 & m_3 \end{pmatrix} \equiv (-1)^{j_1 - j_2 - m_3} (2j_3 + 1)^{-1/2} \langle j_1 m_1, j_2 m_2 | j_1 j_2 \; j_3 \; -m_3 \rangle.
$$

The inner product on the right side are Clebsch-Gordan coefficients. These coefficients vanish unless the quantum numbers satisfy the following conditions:

$$m_1 + m_2 + m_3 = 0,$$
$$|j_1 - j_2| \leq j_3 \leq j_1 + j_2. \tag{A.1}$$

The Wigner $3j$ symbols obey many symmetry properties. Under an even permutation of columns the value remains unchanged; an odd permutation multiplies the value by a factor of $(-1)^{j_1+j_2+j_3}$. The values of the m_i can all change signs by multiplying by the same factor.

$$\begin{pmatrix} j_1 & j_2 & j_3 \\ m_1 & m_2 & m_3 \end{pmatrix} = \begin{pmatrix} j_2 & j_3 & j_1 \\ m_2 & m_3 & m_1 \end{pmatrix} = \begin{pmatrix} j_3 & j_1 & j_2 \\ m_3 & m_1 & m_2 \end{pmatrix}$$

$$(-1)^{j_1+j_2+j_3} \begin{pmatrix} j_1 & j_2 & j_3 \\ m_1 & m_2 & m_3 \end{pmatrix} =$$

$$\begin{pmatrix} j_2 & j_1 & j_3 \\ m_2 & m_1 & m_3 \end{pmatrix} = \begin{pmatrix} j_3 & j_2 & j_1 \\ m_3 & m_2 & m_1 \end{pmatrix} = \begin{pmatrix} j_1 & j_3 & j_2 \\ m_1 & m_3 & m_2 \end{pmatrix}$$

$$\begin{pmatrix} j_1 & j_2 & j_3 \\ m_1 & m_2 & m_3 \end{pmatrix} = (-1)^{j_1+j_2+j_3} \begin{pmatrix} j_1 & j_2 & j_3 \\ -m_1 & -m_2 & -m_3 \end{pmatrix}$$

They also have orthogonality properties as follows:

$$\sum_{j_3,m_3} (2j_3 + 1) \begin{pmatrix} j_1 & j_2 & j_3 \\ m_1 & m_2 & m_3 \end{pmatrix} \begin{pmatrix} j_1 & j_2 & j_3 \\ m_1' & m_2' & m_3 \end{pmatrix} = \delta_{m_1,m_1'} \delta_{m_2,m_2'},$$

$$\sum_{m_1,m_2} \begin{pmatrix} j_1 & j_2 & j_3 \\ m_1 & m_2 & m_3 \end{pmatrix} \begin{pmatrix} j_1 & j_2 & j_3' \\ m_1 & m_2 & m_3' \end{pmatrix} = (2j_3 + 1)^{-1} \delta_{j_3,j_3'} \delta_{m_3,m_3'} \delta(j_1 j_2 j_3),$$

where $\delta(j_1 j_2 j_3) = 1$ if the angular momenta satisfy the triangular condition (A.1) and zero otherwise.

This thesis makes extensive use of the following Wigner $3j$ symbol.

$$\begin{pmatrix} J & J & 2 \\ M & -M & 0 \end{pmatrix} = (-1)^{J-M} \frac{2[3M^2 - J(J+1)]}{[(2J+3)(2J+2)(2J+1)(2J)(2J-1)]^{1/2}}$$

A.2 Wigner $\mathcal{D}$ Functions

The Euler angles (α, β, γ) are a set of angles that rotate one frame of reference S into a new frame S'''. Respectively, these rotations are about the z-axis, y'-axis, and then the z''-axis. The generator of finite rotations for these angles is represented

$$D(\alpha, \beta, \gamma) = \exp\left(\frac{i\alpha}{\hbar}J_z\right) \cdot \exp\left(\frac{i\beta}{\hbar}J_y\right) \cdot \exp\left(\frac{i\gamma}{\hbar}J_z\right).$$

The azimuthal angles α and γ each extend from $(0, 2\pi)$, and the polar angle β extends from $(0, \pi)$. The three Euler angles are denoted by a single symbol ω. The measure is $d\omega = \sin\theta \, d\phi \, d\theta \, d\chi$ and the total solid angle is $8\pi^2$. The matrix elements of the Wigner $D(\omega)$ between two angular momentum states define the Wigner $\mathcal{D}$ functions.

$$\langle jm'| D(\omega) |jm\rangle \equiv \mathcal{D}^{(j)}_{m'm}(\omega)$$

The angular momentum states are in representations that are diagonal in J_z, so the dependence of the Wigner $\mathcal{D}$ functions on the angles α and γ can be immediately expressed.

$$\mathcal{D}^{(j)}_{m'm}(\omega) = \exp(i\alpha m') \, d^{(j)}_{m'm}(\beta) \, \exp(i\gamma m)$$

The β dependence is non-trivial and I denote it with the function $d^{(j)}_{m'm}(\beta)$.

$$d^{(j)}_{m'm}(\beta) = \langle jm'| \exp\left(\frac{i\beta}{\hbar}J_y\right) |jm\rangle = \mathcal{D}^{(j)}_{m'm}(0, \beta, 0)$$

35

The $d_{m'm}^{(j)}(\beta)$ obey the following transformation properties:

$$
\begin{aligned}
d_{m'm}^{(j)}(\pi - \beta) &= (-1)^{j-m'} d_{-m'm}^{(j)}(\pi - \beta) = (-1)^{j-m'} d_{m,-m'}^{(j)}(\beta) \ , \\
d_{m'm}^{(j)}(\beta) &= (-1)^{m'-m} d_{-m',-m}^{(j)}(\beta) = (-1)^{m'-m} d_{m,m'}^{(j)}(\beta) \ .
\end{aligned}
$$

The Wigner $\mathcal{D}$ functions form a complete set of orthonormal functions over the Euler angles.

$$
\frac{1}{8\pi^2} \iiint d\omega \ \mathcal{D}_{m_1',m_1}^{(j_1)*}(\omega) \mathcal{D}_{m_2',m_2}^{(j_2)}(\omega) = \frac{1}{2j_1+1} \delta_{j_1,j_2} \delta_{m_1',m_2'} \delta_{m_1,m_2}
$$

I use the symmetric expression for the integral of the product of three Wigner $\mathcal{D}$ functions to arrive at the result (4.1). This is the general expression:

$$
\frac{1}{8\pi^2} \iiint d\omega \ \mathcal{D}_{m_1',m_1}^{(j_1)}(\omega) \mathcal{D}_{m_2',m_2}^{(j_2)}(\omega) \mathcal{D}_{m_3',m_3}^{(j_3)}(\omega) =
$$

$$
\begin{pmatrix} j_1 & j_2 & j_3 \\ m_1' & m_2' & m_3' \end{pmatrix} \begin{pmatrix} j_1 & j_2 & j_3 \\ m_1 & m_2 & m_3 \end{pmatrix} .
$$

Bibliography

[1] S. Zaheer, S. J. Rahi, T. Emig, and R. L. Jaffe, "Casimir interactions of an object inside a spherical metal shell," *Phys. Rev.*, vol. A81, p. 030502, 2010.

[2] H. B. G. Casimir, "On the Attraction Between Two Perfectly Conducting Plates," *Indag. Math.*, vol. 10, pp. 261–263, 1948.

[3] H. B. G. Casimir and D. Polder, "The Influence of retardation on the London-van der Waals forces," *Phys. Rev.*, vol. 73, pp. 360–372, 1948.

[4] T. Emig, N. Graham, R. L. Jaffe, and M. Kardar, "Casimir forces between arbitrary compact objects," *Phys. Rev. Lett.*, vol. 99, p. 170403, 2007.

[5] T. Emig, N. Graham, R. L. Jaffe, and M. Kardar, "Casimir Forces between Compact Objects: I. The Scalar Case," *Phys. Rev.*, vol. D77, p. 025005, 2008.

[6] S. J. Rahi, T. Emig, N. Graham, R. L. Jaffe, and M. Kardar, "Scattering Theory Approach to Electrodynamic Casimir Forces," *Phys. Rev.*, vol. D80, p. 085021, 2009.

[7] *The Theory and Practice of Fluctuation-Induced Interactions*, (http://online.itp.ucsb.edu/online/fluctuate08/), 2008.

[8] A. R. Edmonds, *Angular Momentum in Quantum Mechanics*. Princeton University Press, 1960.

[9] G. Herzberg, *Molecular Spectra and Molecular Structure, Vol. I: Spectra of Diatomic Molecules*. Van Nostrand Reinhold Company, 1950.

[10] J. Brown and A. Carrington, *Rotational Spectroscopy of Diatomic Molecules*. Cambridge University Press, 2003.

[11] A. Bohr and B. R. Mottelson, *Nuclear Structure, Vols. I & II*. World Scientific Publishing Company, 1975.

[12] S. A. McDowell and W. J. Meath, "Average energy approximations for anisotropic triple-dipole dispersion energy coefficients using three-body interactions involving o2, no, co, n2, h2, and the rare gases as tests," *Canadian Journal of Chemistry*, vol. 76, no. 4, pp. 483–489, 1998.

[13] J. Oddershede and E. N. Svendsen, "Dynamic polarizabilities and raman intensities of co, n2, hcl and cl2," *Chemical Physics*, vol. 64, no. 3, pp. 359 – 369, 1982.

[14] K. P. Huber and G. Herzberg, *Molecular Spectra and Molecular Structure, Vol. I: Constants of Diatomic Molecules*. Van Nostrand Reinhold Company, 1979.